



## Biological Applications of Biosilica/Silk Fibroin/Polyurethane (1:3:1) Composite

P. SUPRIYA PRASAD<sup>1,\*</sup>, T. GOMATHI<sup>2,\*</sup>, P.N. SUDHA<sup>2</sup>, M. DEEPA<sup>1,\*</sup>, J. ANNIE KAMALA FLORENCE<sup>3</sup>,  
A. MUBASHIRUNNISA<sup>4</sup> and SRINIVASAN LATHA<sup>5</sup>

<sup>1</sup>PG and Research Department of Chemistry, Muthurangam Government Arts College (Affiliated to Thiruvalluvar University), Vellore-632002, India

<sup>2</sup>PG and Research Department of Chemistry, D.K.M. College for Women (Affiliated to Thiruvalluvar University), Vellore-632001, India

<sup>3</sup>Department of Chemistry, Voorhees College (Affiliated to Thiruvalluvar University), Vellore-632001, India

<sup>4</sup>Department of Chemistry, Sri Krishna College of Engineering, Arakkonam-631003, India

<sup>5</sup>School of Advanced Science, Vellore Institute of Technology, Vellore-632014, India

\*Corresponding authors: E-mail: drgoms1@gmail.com; deeparam79@gmail.com

Received: 31 January 2022;

Accepted: 5 June 2022;

Published online: 15 June 2022;

AJC-20870

High availability and several benefits of biosilica (BS) in various industries, it becomes a desirable material for industrial purposes. This study is focused to prepare a biocomposite of biosilica isolated from sugarcane baggase and combined with silk fibroin (SF) and polyurethane (PUF) foam. FTIR, XRD, TGA, DSC and SEM measurements were used to characterize the synthesized BS/SF/PUF biocomposite. The potentiality of biosilica composite as an antimicrobial support material was investigated. The BS/SF/PUF biocomposite has a rough surface nature, amorphous and higher thermal stability due to strong contacts, according to the characterization data. Furthermore, the results revealed that the produced material exhibited excellent antioxidant and antimicrobial properties.

**Keywords:** Biocomposite, Biosilica, Silk Fibroin, Polyurethane, Antioxidant property, Antimicrobial activity.

### INTRODUCTION

The use of polymers as biomaterials has a significant impact on medical progress. Biodegradable polymeric biomaterials, in particular, offer the advantages of being able to be broken down and removed after they have served their purpose. Degradable polymers are employed in a variety of clinical settings, including surgical sutures and implants [1]. Materials with desired physical, chemical, biological, biomechanical and degrading qualities must be chosen to meet functional demands. The extraction of sodium silicate from sugarcane bagasse ash has been the subject of extensive research [2-4]. Sugarcane bagasse ash is a waste product from the sugar industry as well as a byproduct from a biopower plant.

The extracted biosilica was combined with silk fibroin and polyurethane foam to prepare a biocomposite which could be active against selected microorganisms. Silk fibroin, a naturally occurring protein produced by the domestic silkworm, *Bombyx mori* [5] has been recognized as a potentially useful

biomaterial. Three chain units such as heavy, light and a P25 glycoprotein make up the *Bombyx mori* silkworm [6,7]. GAGAGS repeats and GAGAGX (X = V or Y) repeats are heavy and light chain units [8]. These repeating units tend the silk fibroin to self-assemble into antiparallel -sheet structures via hydrogen bonds and van der Waals interactions [9]. The material is used till date for its superior properties like robustness, lustre, resilience, ability to conform to the surface of molds, ease of manipulation and ability to bind with chemical dyes. It is also recognized for its applications in the field of medicine [10].

Polyurethanes (PUs) are a type of polymer that is widely employed in the medical device sector. The presence of hard and soft segments in their chemical structure confers elasticity and mechanical strength to the polymer [11]. They are preferred in the manufacture of heart valves, blood vessels, vascular grafts and catheters due to their elastomeric properties and good blood compatibility [12-14].

Hence, in present study, the ternary biocomposite of biosilica/silk fibroin/polyurethane (BS/SF/PUF) foam was pre-

pared and characterized using FTIR, XRD, TGA, DSC and SEM analysis. The prepared biocomposite was evaluated for its antioxidant and antimicrobial properties, which can be used as a good wound healing material. Furthermore, the development of novel surfaces that restrict biofilm formation by the release of antimicrobial agents, contact-killing, microbial adhesion inhibition and biofilm disruption has been recommended as a way to lower the prevalence of device-associated infections.

## EXPERIMENTAL

Raw silk fibers (cocoons of *Bombyx mori*) were purchased from a local sericulture farm situated in Vaniyambadi, India. Sugarcane bagasse was provided from a local cane-sugar mill in Vellore, India. Polyurethane ( $\rho_{\text{bulk}} = 0.08 \text{ g/cm}^3$ ) and glutaraldehyde (25% aqueous solution) were procured from Sigma Aldrich, India. All chemicals were of analytical grade and used directly in the experimental works. Milli-Q ultrapure water ( $18.2 \text{ M}\Omega \text{ cm}$ ,  $\leq 5 \text{ ppb}$ ) was used for all aqueous applications.

**Preparation of biosilica/silk fibroin/polyurethane foam biocomposite:** Ternary biopolymer composite was prepared by combining biosilica (BS), silk fibroin (SF) and polyurethane (PUF) in the mass ratio of 1:3:1. The solid mixture system was dissolved in 100 mL of formic acid. Subsequently, the prepared biocomposite was poured in a petridish and was allowed to dry at room temperature. Finally, the as-synthesized biocomposite film was milled at 500 rpm to obtain the BS/SF/PUF sorbent and stored in air tight containers for further use.

**Characterization:** Infrared analysis of the prepared BS/SF/PUF biocomposite was determined using a Perkin-Elmer 200 FTIR spectrophotometer in the range of  $4000\text{--}400 \text{ cm}^{-1}$ . The phase purity and crystallinity percentage of the prepared biocomposite was studied using a Shimadzu XRD-7000 diffractometer with Ni filter  $\text{CuK}\alpha$  radiation source for  $10^\circ/\text{min}$  scan rate at 40 kV and 30 mA. The average crystalline sizes were calculated by Debye-Scherrer equation. Thermal behaviour of the biocomposite was investigated using Perkin-Elmer TGA 8000 equipment in the range of 25 to  $800^\circ\text{C}$  under a nitrogen flow rate of  $50 \text{ mL/min}$ . The surface morphology of the prepared biocomposite was evaluated using Hitachi-S-3400N scanning electron microscope. The DSC investigations of the readied tests were done utilizing DSC Q10 V 9.0 Build 275 instrument with the temperature range between 30 to  $350^\circ\text{C}$  at the warming pace of  $10^\circ\text{C/min}$ .

**Antioxidant assay:** The antioxidant studies were conducted using the DPPH free radical scavenging assay. The assay was executed by mixing the prepared biocomposites ( $20\text{--}120 \mu\text{g/mL}$ ) with 4 mL of DPPH (0.004% methanolic solution) and then incubated for 0.5 h at room temperature. After the completion of incubation, the radical scavenging potential of biocomposite was investigated by calculating the decrease in absorbance of DPPH from 517 nm. The control used was a blank solution of DPPH. The percentage of scavenging was calculated using the equation given below:

$$\text{Scavenging activity (\%)} = \frac{A_c - A_s}{A_c} \times 100$$

where  $A_c$  = absorbance of the control;  $A_s$  = absorbance of the solution containing the biocomposite.

**Antimicrobial activity:** The antimicrobial activity of the prepared biocomposite BS/SF/PUF was tested against three bacterial and three fungal strains by the Agar-well diffusion method with the help of Muller-Hinton Agar (MHA) medium. The bacterial strains used in the current work were *Bacillus* sp. (Gram-positive), *Klebsiella* sp. and *Proteus* sp. (Gram-negative) and the fungal strains used were *Rhizopus* sp., *Aspergillus niger* and *Candida* sp. Initially, the microorganisms were inoculated on the MHA medium. A sterile spreader was used to spread it evenly. The MHA medium was allowed to congeal. A small quantity of biocomposite BS/SF/PUF prepared was placed on different cultured agar plates. For the diffusion of biocomposite, the plates were allowed to stay undisturbed for 1 h at room temperature. Before the initiation of growth of the microorganisms, the plates were kept on different racks for 24 h at  $37^\circ\text{C}$  for incubation. Both antibacterial and antifungal activities of the prepared biocomposite were ascertained by estimating diameter of the zone of inhibition grown around the discs against the microorganisms using the measuring scale.

## RESULTS AND DISCUSSION

**FTIR analysis:** The presence of multifunctional groups in synthesized BS/SF/PUF composite was investigated by FTIR analysis. Fig. 1 illustrates the FTIR spectrum of BS/SF/PUF composite of ratio 1:3:1. The broad band appeared at around  $3433 \text{ cm}^{-1}$  indicates the presence of  $-\text{OH}$  and  $-\text{NH}$  groups associated with hydrogen bonding [15]. The absorption band due to C-H stretching vibrations appeared at  $2904 \text{ cm}^{-1}$  while the vibrations at  $1656 \text{ cm}^{-1}$  corresponded to the carbonyl bands ( $\text{C}=\text{O}$ ) of PUF and the band appeared at  $1577 \text{ cm}^{-1}$  could be associated with the  $-\text{NH}$  bending of amide group contained in the SF structure. These findings demonstrated that the SF and PUF of biocomposite were successfully combined with the BS. Furthermore, the characteristic Si-O-Si group and Si-O group of the BS stretching vibrations showed a blue shift of their peaks to  $1082$  and  $800 \text{ cm}^{-1}$ , respectively, confirming the successful interactions between the different functional groups of BS with those of SF and PUF during composite formation.

The Si-O-Si symmetric stretching vibration at  $455\text{--}450 \text{ cm}^{-1}$  and the Si-O-Si asymmetric stretching vibration at  $1090\text{--}$

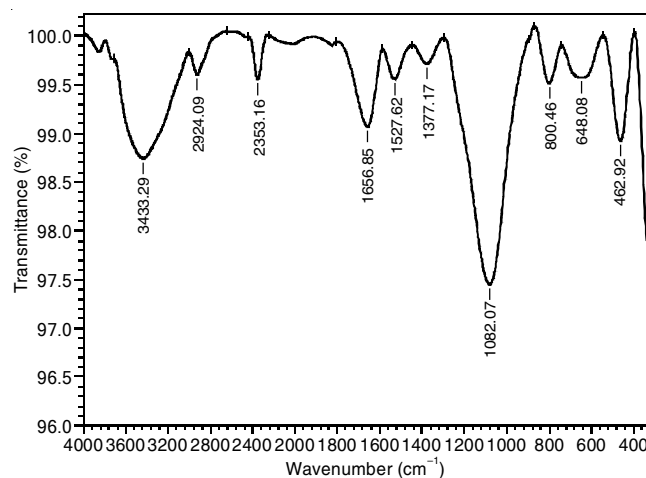


Fig. 1. FTIR spectrum of BS/SF/PUF composite

1050  $\text{cm}^{-1}$  were detected in the spectra [16]. A random assembly of a  $\text{Si}(\text{OH})_4^+$  unit forms the bulk structure of amorphous silica. Fundamental Si-O vibrations are attributed to three strong absorption bands identified in FTIR measurements at 800.46, 1082.07 and 1377.17  $\text{cm}^{-1}$  [4]. On comparing the FTIR spectrum of BS (spectrum not given) and BS/SF/PUF composite, the band position of main function groups such as OH and C=O of BS was shifted from 3648 to 3433  $\text{cm}^{-1}$  and 1656 to 1647  $\text{cm}^{-1}$ , respectively in BS/SF/PUF biocomposite.

**XRD analysis:** XRD pattern of BS/SF/PUF is shown in Fig. 2. The XRD pattern exhibits one broad peak at  $2\theta = 21.7^\circ$  along with the shoulder peak  $26.9^\circ$ . Appearance of broad peaks reveals the amorphous phases of the prepared BS/SF/PUF biocomposite. Also the broadening of the peaks is due to the increase of strong interaction between the functional groups present in the polymers. The hydrogen bond formed between the OH and NH functional groups are the main contribution of destroyed regularity and leads to the amorphous phases while mixing biosilica (BS), silk fibroin (SF) and polyurethane (PUF).

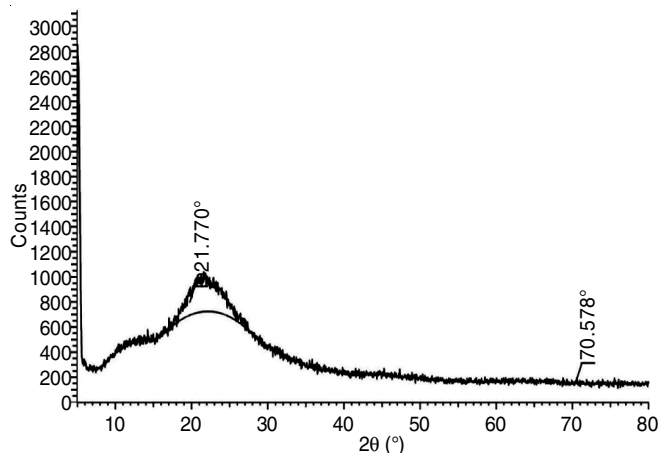


Fig. 2. XRD pattern of BS/SF/PUF biocomposite

While mixing the polymers, the crystalline peaks of the individual polymers get destroyed and the new long broad peak appeared for the prepared biocomposite. The presence of amorphous nature is an essential criterion for cell attachment and proliferation. The amorphous phase of the biomaterial facilitates favourable medium for the new cells to develop. Hence, it is expected that the BS/SF/PUF biocomposite will be a suitable wound healing material.

**TGA analysis:** The change in the rate of weight loss of material as the function of temperature or time was measured using thermogravimetric analysis in a controlled atmosphere. The TGA thermogram of BS/SF/PUF biocomposite is depicted in Fig. 3, which shows two decomposition stages. In first stage of decomposition, about 5% weight loss had taken place from 30 to 150 °C. Followed this maximum weight loss of about 16.65% was observed in the second stage. This was due to the breakage and elimination of small molecules from the prepared biocomposite. At the end of the experiment about 78% of the sample remains as residue. This revealed the higher thermal stability of the prepared biocomposite.

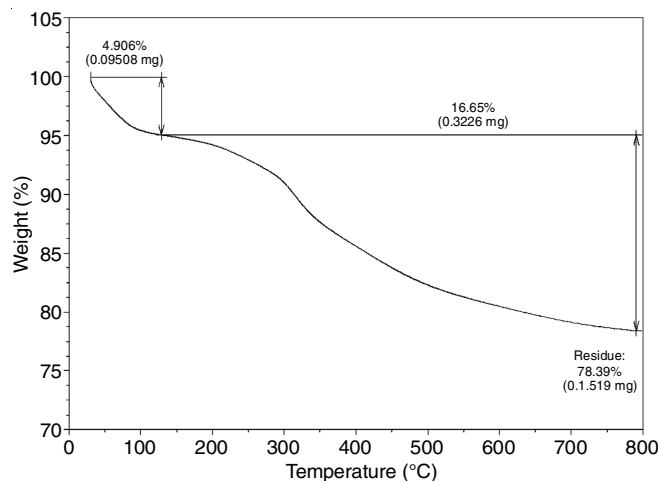


Fig. 3. TGA thermogram of BS/SF/PUF biocomposite

**DSC analysis:** In the temperature range of 25 to 425 °C, the DSC curve demonstrates typical endothermic behaviour of BS/SF/PUF biocomposite (Fig. 4). Biomass decomposition was steady and somewhat exothermic at temperatures more than 425 °C. The complicated composition of biomass and its behaviour during thermal degradation are likely to have caused this outcome for the DSC profile. A broad endothermic peak at 195 °C were attributed to the elimination of absorbed water associated with the hydrophilic groups of the biopolymer and a sharp exothermic peaks at 625 °C are attributed to the decomposition of side chains of ternary BS/SF/PUF biocomposite (Fig. 4).

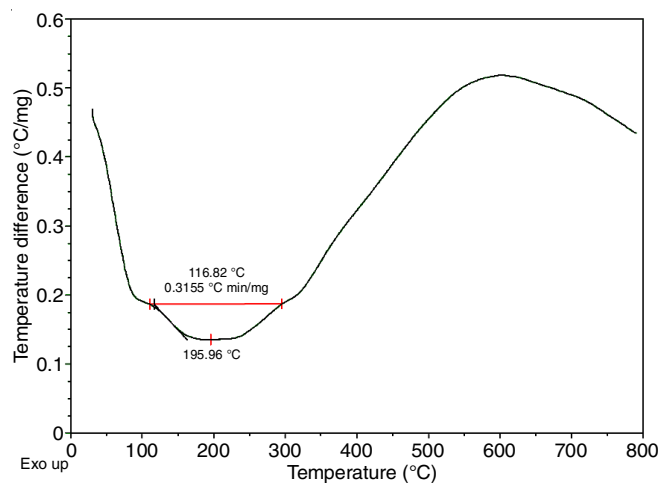


Fig. 4. DSC thermogram of BS/SF/PUF biocomposite

According to Yang *et al.* [17], DSC endothermic values exhibit low and steady profiles at around 250 °C, with a small attenuation between 275 and 300 °C, which could be due to the endothermic nature breakdown. The DSC endothermic profile grew beyond 300 °C until it reached 360 °C, which can be explained by volatilization peak. The glass transition temperature for the ternary scaffold is 535 °C. A material's long-term thermal stability will be greater if its  $T_g$  is higher. The ternary structure is thermally more stable. The BS/SF/PUF biocomposite was also found to be extremely thermally stable

glass transition temperature and proved to be the most promising materials to carry out tissue engineering based on the obtained higher onset temperature and higher value of glass transition temperature.

**SEM analysis:** SEM images were obtained to evaluate the microstructure morphology of BS/SF/PUF biocomposite (Fig. 5). An open porous structure network was observed for BS/SF/PUF biocomposite. High porosity and pore structures that were evenly dispersed [18]. The addition of BS and PUF to SF introduced an impact on porosity and pore structure [19]. The variation in pore architecture is due to the polymeric homogeneity. The functional groups such as –OH and –NH present in SF and PUF participates in the H-bond interactions.

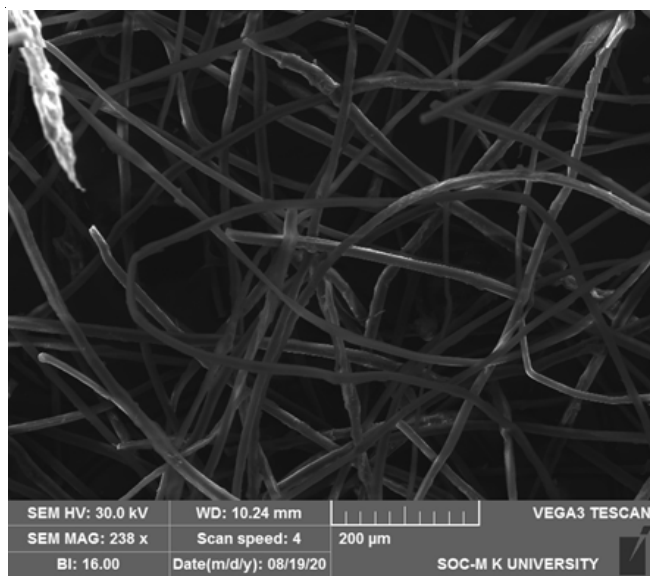


Fig. 5. SEM image of BS/SF/PUF biocomposite

Microstructural characteristics such as microporosity or surface roughness are preferred for cell–composite interactions [20]. As a result, it was suggested that the BS/SF/PUF biocomposite exhibited strongly linked pores with the characteristic reticulated structure. As a result of the characterization, the exceptional relationship generated between SF, BS and PUF is revealed.

**Antimicrobial activity:** *Bacillus sp.*, *Klebsiella sp.* and *Proteus sp.* were used to investigate the bioefficacy of BS/SF/PUF (1:3:1) biocomposite. Fig. 6 shows the zone of inhibition values of ternary BS/SF/PUF composite against specified microorganisms. The zone of inhibition values displayed by the BS/SF/PUF composite against the growth of the selected *Bacillus sp.*, *Klebsiella sp.* and *Proteus sp.* were found to be 15 mm, 14 mm and 13 mm, respectively. The results worth mentioning that the ternary composite is effective not only against Gram-positive bacteria with a single cytoplasmic membrane, but also against Gram-negative bacteria with two bilayers, such as the outer and inner cytoplasmic membranes. As a result, it is clear that the prepared BS/SF/PUF composite has good antibacterial action.

*Rhizopus sp.*, *Aspergillus niger* and *Candida sp.* were used to investigate the antifungal activity of the prepared BS/SF/

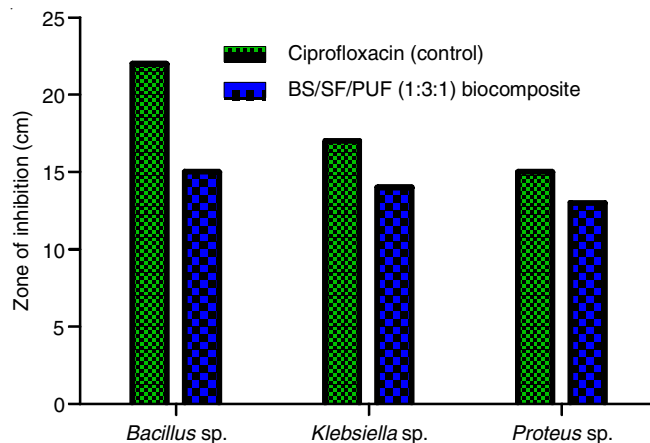


Fig. 6. Antibacterial activity of BS/SF/PUF composite

PUF (1:3:1) biocomposite. The zone of inhibition values 4, 7 and 9 mm was displayed by the BS/SF/PUF composite against selected microorganisms respectively (Fig. 7). The biocomposite prepared was directly placed on the agar plates for antifungal activities and the significant activities of the samples were compared. The findings suggested that polymeric surfaces can be efficiently changed and turned into antimicrobial surfaces, hence a stronger affinity for bacteria and fungi and more antimicrobial action.

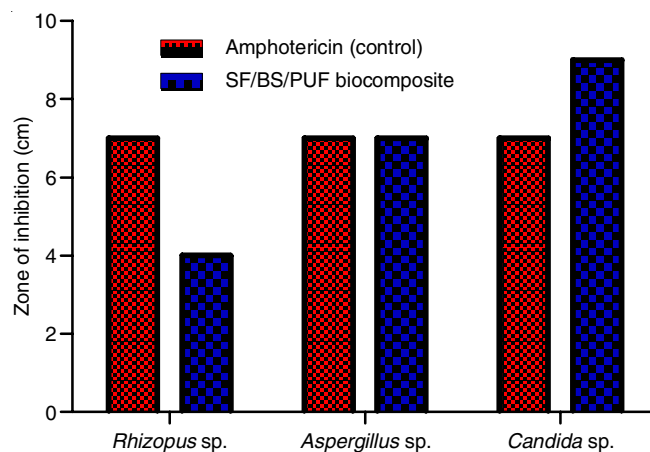


Fig. 7. Antifungal activity of BS/SF/PUF biocomposite

**Antioxidant activity:** The percentage of DPPH radical scavenging activity of various concentrations of BS/SF/PUF ternary composite is shown in Fig. 8. At various doses, such as 20, 40, 60, 80, 100 and 120  $\mu\text{g/mL}$ , the DPPH free radical scavenging activity was studied. The experimental data revealed that as the concentration of BS/SF/PUF ternary biocomposite increases, so does the scavenging percentage. The absorbance measured at 517 nm decreases as the concentration of BS/SF/PUF ternary composite produced is increased from 20  $\mu\text{g/mL}$  to 120  $\mu\text{g/mL}$ , showing a higher free radical scavenging activity from 69% to 99%. The purple tint of the DPPH solution fades quickly as it comes into contact with proton-radical scavengers [21].

The highest free radical scavenging activity demonstrates that the BS/SF/PUF ternary composite has good antioxidant activity, which is beneficial to the cells' ability to multiply,

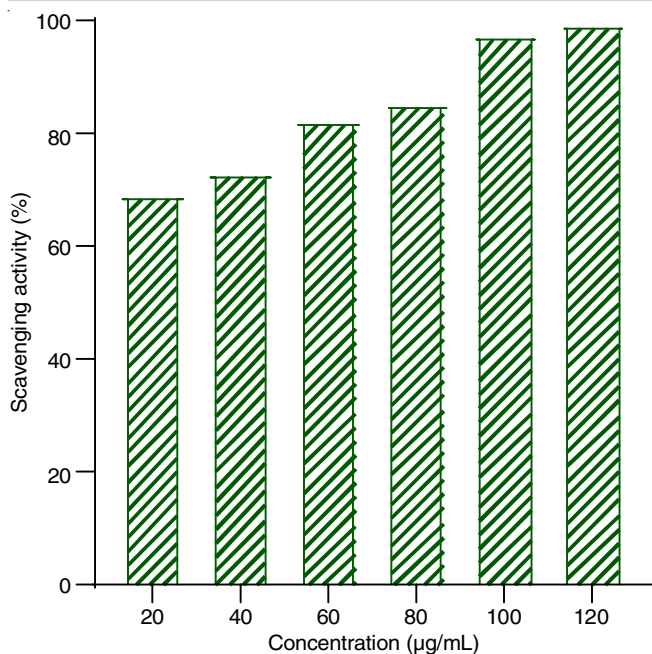


Fig. 8. Antioxidant activity of BS/SF/PUF biocomposite

differentiate and create specific tissues. These findings point to the potential benefits of using SF and PUF [22]. Hence, the overall results revealed that the BS/SF/PUF biocomposite can have soft tissue ion augmentation and wound healing, as well as biological functions such as antioxidant, antimicrobial and anti-inflammatory properties, without the need for a long clinical period.

## Conclusion

The present work was mainly aimed to prepare and characterize biosilica/silk fibroin/polyurethane foam (BS/SF/PUF) biocomposite. The characterization of BS/SF/PUF biocomposite were performed using suitable techniques such as FTIR, TGA, DSC, XRD and SEM analyses. The FTIR spectrum showed characteristic bands of all the materials used, thus proving strong interaction between all the components used. TGA and DSC thermograms showed better thermal stability of the prepared BS/SF/PUF biocomposite. SEM studies revealed that the high surface area and porous structure with providing good adsorbability, which can facilitate the cell adhesion. A better antibacterial and antifungal activity of the prepared biocomposite heaps on the microbial cell exterior as the physiological pH in microbial cells.

## CONFLICT OF INTEREST

The authors declare that there is no conflict of interests regarding the publication of this article.

## REFERENCES

1. T. Hoshiba, T. Orui, C. Endo, K. Sato, A. Yoshihiro, Y. Minagawa and M. Tanaka, *RSC Adv.*, **6**, 89103 (2016); <https://doi.org/10.1039/C6RA15229E>
2. Megawati, D.S. Fardhyanti, R.D. Artanti Putri, O. Fianti, A.F. Simalango and A.E. Akhir, *MATEC Web Conf.*, **237**, 2002 (2018); <https://doi.org/10.1051/mateconf/201823702002>
3. S. Norsuraya, R. Norhasyimi and H. Fazlena, *Malays. J. Anal. Sci.*, **21**, 512 (2017); <https://doi.org/10.17576/mjas-2017-2102-26>
4. P. Chindaprasirt and U. Rattanasak, *Sci. Rep.*, **10**, 9890 (2020); <https://doi.org/10.1038/s41598-020-66885-y>
5. T.P. Nguyen, Q.V. Nguyen, V.-H. Nguyen, T.-H. Le, V.Q.N. Huynh, D.-V.N. Vo, Q.T. Trinh, S.Y. Kim and Q.V. Le, *Polymers*, **11**, 1933 (2019); <https://doi.org/10.3390/polym11121933>
6. A.B. Mathur and V. Gupta, *Nanomedicine*, **5**, 807 (2010); <https://doi.org/10.2217/nnm.10.51>
7. Y. Qi, H. Wang, K. Wei, Y. Yang, R.-Y. Zheng, I.S. Kim and K.-Q. Zhang, *Int. J. Mol. Sci.*, **18**, 237 (2017); <https://doi.org/10.3390/ijms18030237>
8. F. Mottaghitlab, M. Farokhi, M.A. Shokrgozar, F. Atyabi and H. Hosseinkhani, *J. Control. Rel.*, **206**, 161 (2015); <https://doi.org/10.1016/j.jconrel.2015.03.020>
9. F. Philipp Seib, *AIMS Bioeng.*, **4**, 239 (2017); <https://doi.org/10.3934/bioeng.2017.2.239>
10. C. Belbéoch, J. Lejeune, P. Vroman and F. Salaün, *Environ. Chem. Lett.*, **19**, 1737 (2021); <https://doi.org/10.1007/s10311-020-01147-x>
11. I. Francolini, F. Crisante, A. Martinelli, L. D'Ilario and A. Piozzi, *Acta Biomater.*, **8**, 549 (2012); <https://doi.org/10.1016/j.actbio.2011.10.024>
12. F.M. Carvalho, F.J.M. Mergulhão and L.C. Gomes, *Antibiotics*, **10**, 1525 (2021); <https://doi.org/10.3390/antibiotics10121525>
13. M. Pergal and M. Balaban, Eds.: G. Rohman, Synthesis and Structure-Property Relationships of Biodegradable Polyurethanes, In: Biodegradable Polymers: Recent Developments and New Perspectives, IAPC Publishing, Zagreb, Croatia, Chap. 5, pp. 141-190 (2017).
14. Z. Petrovic, I. Javni and M. Ionescu, *J. Renew. Mater.*, **1**, 167 (2013); <https://doi.org/10.7569/JRM.2013.634112>
15. M.O. Kareem, A.A. Edathil, K. Rambabu, G. Bharath, F. Banat, G.S. Nirmala and K. Sathiyarayanan, *Chem. Eng. Commun.*, **208**, 801 (2021); <https://doi.org/10.1080/00986445.2019.1650034>
16. R.H. Alves, T.V. da S. Reis, S. Rovani and D.A. Fungaro, *J. Chem.*, **2017**, 6129035 (2017); <https://doi.org/10.1155/2017/6129035>
17. H. Yang, R. Yan, H. Chen, D.H. Lee and C. Zheng, *Fuel*, **86**, 1781 (2007); <https://doi.org/10.1016/j.fuel.2006.12.013>
18. E.M. Charry, M. Neumann, J. Lahti, R. Schennach, V. Schmidt and K. Zojer, *J. Microsc.*, **272**, 35 (2018); <https://doi.org/10.1111/jmi.12730>
19. E. Capuana, F. Lopresti, F. Carfi Pavia, V. Brucato and V. La Carrubba, *Polymers*, **13**, 2041 (2021); <https://doi.org/10.3390/polym13132041>
20. N. Abbasi, S. Hamlet, R.M. Love and N.-T. Nguyen, *J. Sci. Adv. Mater. Devices*, **5**, 1 (2020); <https://doi.org/10.1016/j.jsamd.2020.01.007>
21. S.M. Elbayomi, H. Wang, T.M. Tamer and Y. You, *Polymers*, **13**, 2575 (2021); <https://doi.org/10.3390/polym13152575>
22. S. Roy and J.-W. Rhim, *Int. J. Biol. Macromol.*, **162**, 1780 (2020); <https://doi.org/10.1016/j.ijbiomac.2020.08.094>